Effects of Chain Length and Electrolyte on the Adsorption of n-Alkylpyridinium Bromide Surfactants at Sand-Water Interfaces

ARTICLE *in* INDUSTRIAL & ENGINEERING CHEMISTRY RESEARCH · JANUARY 2006

Impact Factor: 2.59 · DOI: 10.1021/ie050808y · Source: OAI

2 AUTHORS, INCLUDING:

Santanu Paria
National Institute of Technology Rourkela
52 PUBLICATIONS **1,778** CITATIONS

Effects of Chain Length and Electrolyte on the Adsorption of *n*-Alkylpyridinium Bromide Surfactants at Sand−Water Interfaces

Santanu Paria* and Pak K. Yuet

Department of Chemical Engineering, Dalhousie University, P.O. Box 1000, Halifax, Nova Scotia, Canada B3J 2X4

The kinetic and equilibrium studies of the adsorption of four cationic surfactants (pyridinium bromide) with different chain lengths (C_{16}, C_{14}, C_{12}, and C_{10}) onto sand are presented here. The adsorption and desorption behavior in the absence and presence of different electrolytes (NaCl, $CaCl_2$, and Na_2SO_4) are compared in batch and continuous column experiments. The kinetic studies show that the rates of adsorption of pyridinium bromide surfactants on sand surfaces are very high (∼70% of saturation adsorption occurs in 30 s) and are almost the same at low concentration (0.5 mM) for different chain lengths. The amount of surfactant adsorbed is enhanced by the presence of electrolyte because of a reduction in electrostatic repulsion among the headgroups, whereas the effect of the valence of coion does not appear to be important. Desorption studies based on column experiments show that a lower amount of surfactant is retained when eluted with electrolyte solution instead of pure water.

1. Introduction

Adsorption of cationic surfactants at solid/liquid interfaces is of great importance because of a wide range of applications in detergency, wetting, ore flotation, and corrosion inhibition. Cationic surfactants have also been suggested for potential use in the remediation of contaminated soils and aquifers.[1,2] The most common types of groundwater contamination arise from spills of hydrocarbon fuels and solvents, coal storage, and coking sites. These hydrocarbons are trapped inside the soil matrix or adsorbed on soil grains and slowly contaminate groundwater because of their finite solubility in water. In this case, surfactants may be used to clean the soil by solubilizing and removing the trapped organics in the soil matrix.

On the other hand, water contaminated by organics can also be purified by sorption of the organics onto soil from water. The sorption of organic contaminants from water by soil is controlled by the soil organic matter content.[3] Low organic matter soils have very little sorptive capability for common groundwater contaminants. Cationic surfactants can be readily adsorbed onto negatively charged soil grains, resulting in more hydrophobic surfaces, which can, in turn, enhance the removal of organic contaminants from water.[1]

To facilitate the application of surfactant-based technologies in soil and groundwater remediation as well as water purification, it is important to develop a better understanding of surfactant adsorption and desorption on soil. There are many batch adsorption studies of cationic surfactants on different solid−liquid interfaces, such as silica,[4−8] soil and clay,[1,2,9−11] and alumina.[12] The hydrocarbon chain (tail) length has been found to be of critical importance in determining the adsorption behavior of surfactants. It has been reported that, in the case of adsorption of cationic surfactant on silica, increasing the hydrocarbon chain length by four methylene units, from C_{12} to C_{16}, lowers the concentration at which characteristic features of the adsorption isotherm occur by approximately an order of magnitude.[13] Small alkylammonium compounds such as *n*-butylammonium are adsorbed by a cation-exchange mechanism,[14] while alkylammonium compounds with a tail length greater than a critical value (eight carbons) are adsorbed via both cation exchange and hydrophobic bonding.[15]

Xu and Boyd[16] reported that a higher ionic strength and a change of the companion anion from Cl^-, Br^-, or SO_4^{2-} resulted in increased adsorption of quaternary ammonium compounds by hydrophobic bonding. Atkin et al.[7] and Subramanian and Ducker[17] reported that chloride ions have less influence on adsorbed hexadecyltrimethylammonium surfactant structure than bromide ions because of the lower binding efficiency of chloride ions compared to that of bromide ions.

In this paper, we report the results of batch and column studies of adsorption of series cationic surfactants with different tail lengths in the presence and absence of electrolyte. The knowledge of adsorption efficiency on soil and desorption efficiency from soil in an aqueous medium is essential to prevent the loss of surfactant due to adsorption in the remediation of organic contaminants in soil and groundwater. In addition to increased surfactant cost, the presence of high surfactant concentration in the soil and groundwater may contaminate the environment.[18]

2. Materials and Methods

The cationic surfactant cetylpyridinium bromide (C_{16}PB) was obtained from Aldrich Chemicals and was used as received. Tetradecylpyridinium bromide (C_{14}PB), dodecylpyridinium bromide (C_{12}PB), and decylpyridinium bromide (C_{10}PB) were synthesized in our laboratory and were recrystallized five times from acetone before use. The chemical structure of *n*-alkylpyridinium bromides is given in Figure 1. The critical micelle concentrations (CMC) of the surfactants were determined by surface tension measurement and are given in Table 1. ACS grade NaCl, Na_2SO_4, and $CaCl_2$ were purchased from EMD Chemicals, Germany. Ultrapure water of 18.2 MΩ resistivity (Barnstead International) was used for all experiments. The sand used for column studies was obtained from Bonar Inc., Canada. The sand density was determined experimentally to be 2.6 g/cm^3. The sand surface area was 0.3 m^2/g, determined by the

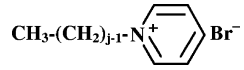

Figure 1. Chemical structure of *n*-alkylpyridinium bromide.

Table 1. Critical Micelle Concentration (CMC) of *n*-Alkylpyridinium Bromide (C_jPB) Surfactants with Different Tail Lengths (j = 16, 14, 12, and 10) at 25 °C

surfactants	CMC (mM)
C_{16}PB	0.9
C_{14}PB	3.5
C_{12}PB	11
C_{10}PB	40

methylene blue adsorption method.[19] The pH_{PZC} (point of zero charge) of sand is reported as ~2, and the charge becomes negative between pH 6 and 11.[20]

2.1. Sand Sieving and Cleaning. The sand was sieved in a sieve shaker and the 212−500 μm sized sand was taken for the experiments. The sand was cleaned prior to each experiment according to the procedure given by Johnson et al.[21] Briefly, the sand was first washed thoroughly with water, followed by immersion in sodium dithionite solution (0.1 M $Na_2S_2O_4$) for 2 h to remove surface metallic compounds such as iron oxide and manganese oxide. Organic impurities were removed by soaking the sand in hydrogen peroxide (5%) for 3 h followed by washing with pure water and subsequent overnight soaking in HCl (12 N). The sand was then rinsed thoroughly with pure water until the pH of the wash water shows the value of pure water (~6.8−7). The cleaned sand was then dried in an oven at 100 °C for 24 h.

2.2. Experimental Measurements. Surfactant concentrations were measured using a UV−visible spectrophotometer (Shimadzu, model UV-1700). The concentrations were determined using a standard linear plot of absorbance vs concentration at 259 nm wavelength (λ_{max}) with quartz glass cells of 10 mm path length. Surface tension was measured by the Wilhelmy plate method using a Kruss K100 tensiometer. Surfactant solutions were prepared by diluting concentrated stock solutions. In the batch studies, the amount of adsorbent (sand) and the volume of solution were kept constant for each set of experiments, in which 10 g of sand and 25 mL surfactant solution were kept in a plastic bottle and the system was stirred slowly (to avoid excessive foaming) using a mechanical shaker. The pH of the experimental solution was measured the same as that of pure water (~6.8−7). The solution was analyzed after being decanted into a glass tube (for kinetic study after a particular time interval and for equilibrium study, after 1 h) and centrifuged at 5000 rpm for 30 min. The amount of surfactant adsorbed (in μmol/g) in the batch was determined as follows: $(C_0 - C_{eq})v/m$, where v is the volume of solution used (in mL), m is the mass of sand in g, and C_0 and C_{eq} are the initial and equilibrium surfactant concentrations (in mM/L), respectively. The amount of surfactant retained in the column (in μmol/g) after elution with pure water or electrolyte solution was determined as follows: $(C_0v_1 - C_2v_2)/m$, where C_0 and C_1 are the initial and final concentrations (in mM/L), respectively, v_1 is the volume of surfactant solution pumped through the column (in mL), v_2 is the total volume of solution collected from the column at the end (in mL), and m is the mass of sand used inside the column (in g). All experiments were performed at room temperature (25 °C). Column experiments were conducted using a glass column with inner threaded poly(tetrafluoroethylene) (PTFE) caps shielded with O rings at both ends. The column was 30 cm in length and 1.5 cm in diameter. A constant flow rate of 3.3 mL/min, controlled using a peristaltic pump

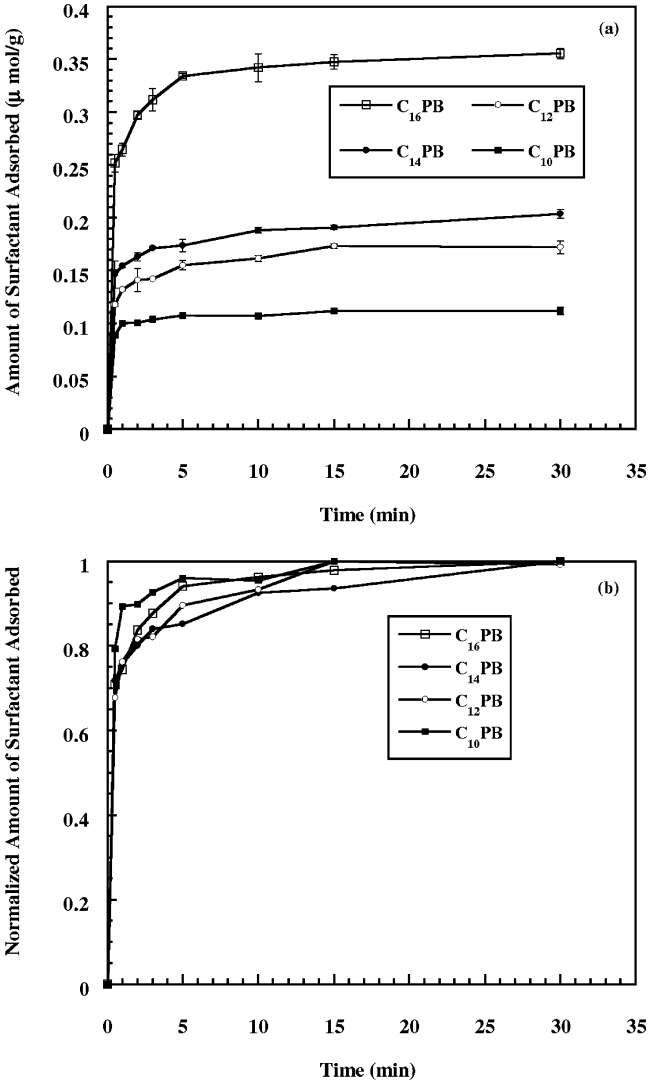

Figure 2. (a) Adsorption kinetics of C_{16}PB, C_{14}PB, C_{12}PB, and C_{10}PB on sand from 0.5 mM initial concentration at 25 °C. (b) Adsorption kinetics of C_{16}PB, C_{14}PB, C_{12}PB, and C_{10}PB; amount adsorbed is normalized by their corresponding saturation amount adsorbed in part a.

(Masterflex, Cole Parmer), was used. The porosity or void fraction, v_p, of the sand bed was 0.42, calculated according to the following relation,

$$v_p = \frac{V - (m/\rho)}{}$$

where V is the empty column volume, m is the mass of the sand used, and ρ is the sand density.

3. Results and Discussion

3.1. Kinetics and Equilibrium Batch Adsorption Studies. The adsorption kinetics of four surfactants with different alkyl chain lengths at the sand−water interface were studied to obtain information on the rate and equilibrium time of adsorption. Figure 2a presents the adsorption kinetics of C_{16}PB, C_{14}PB, C_{12}PB, and C_{10}PB at 0.5 mM concentration. From the figure, it is observed that the rate of adsorption of alkylpyridinium bromide surfactants on sand is very high, with almost 70% of the maximum amount being adsorbed within 30 s for all cases. Figure 2b depicts the adsorption of the four surfactants, normalized by their respective maximum values. The figure shows no significant difference among the four surfactants,

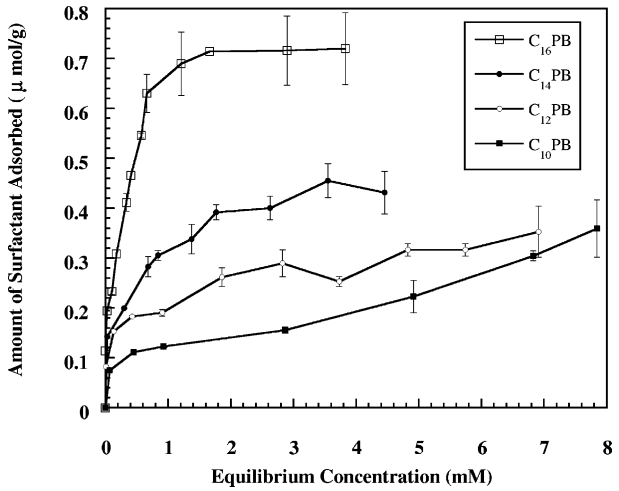

Figure 3. Adsorption isotherms of C_{16}PB, C_{14}PB, C_{12}PB, and C_{10}PB on sand at 25 °C. Plateau of C_{10}PB was not determined, as high dilution ratio required at higher concentration may give error in UV method.

which suggests that the rate of adsorption is almost similar for all the four cases. We hypothesized that the observed results due to the electrostatic interactions play an important role in the adsorption of cationic surfactants on negatively charged sand surfaces at low concentration (0.5 mM) where hydrophobic interaction is less. Figure 3 shows the adsorption isotherms of the four surfactants. Note that the natures of the isotherms are typical four regions, very similar to those reported in the literature.[7,22] In particular, with increasing tail length, the maximum amount adsorbed at saturation increases mainly because of increasing hydrophobic interactions. The hydrophobic interactions include those laterally between the tails of adsorbed molecules at the solid surface, interactions between the tails of adsorbed molecules and that present in solution, and also those between the surfactant tail and surface (when adsorption occur on hydrophobic sites). An increase in chain length is also considered to decrease the Gibbs free energies of the micellization and hemimicellization processes, resulting in a shift of CMC and HMC (hemimicellar concentration) toward lower concentrations.[22]

3.2. Effect of Electrolytes in Batch Studies. The effect of electrolyte on the adsorption of C_{14}PB (0.5 mM) was studied using NaCl, Na_2SO_4, and $CaCl_2$. Figure 4 depicts the variation of specific adsorption as a function of κ, where κ is the Debye−Hückel parameter, defined as

$$\kappa = \left[\frac{1000e^2N_A}{\epsilon_r\epsilon_0 k_B T}\sum_i z_i^2 C_i\right]^{1/2} \quad (2)$$

where e is the elementary charge, N_A is Avogadro's number, ϵ_r is the dielectric constant, ϵ_0 is the permittivity in a vacuum, k_B is the Boltzmann constant, T is the absolute temperature, and z_i and C_i are the valence and molar concentration of ionic species i, respectively. In the case of adsorption of cationic surfactants on negatively charged surfaces, two types of electrostatic interactions play a critical role: (i) that between the surfactant and the solid surface and (ii) that among the surfactant heads. Since electrostatic interaction is weakened by increasing ionic strength, the observation that specific adsorption increases with κ attributes that electrostatic repulsion among surfactant heads is the dominant interaction in determining the adsorption of alkyl-PB on sand surfaces. More specifically, the weakened repulsion allows more molecules to adsorb on the sand surface. Increased hydrophobic bonding also is another reason of

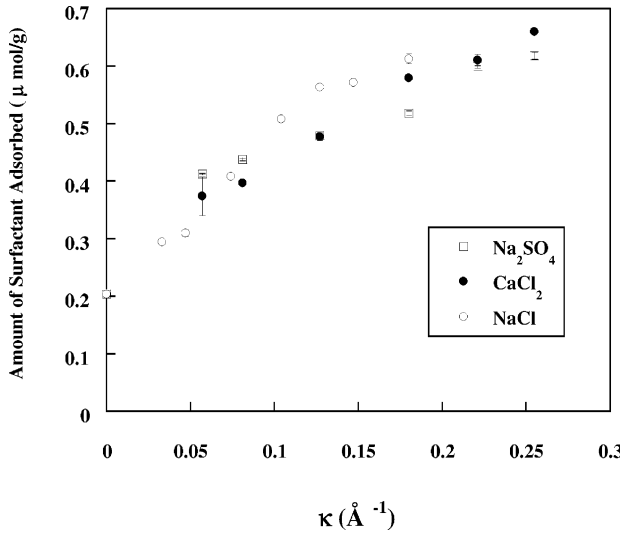

Figure 4. Variation of specific adsorption of C_{14}PB as a function of Debye−Hückel parameter (κ). The initial concentrations of C_{14}PB were 0.5 mM, and the equilibrium time was taken for 1 h at 25 °C.

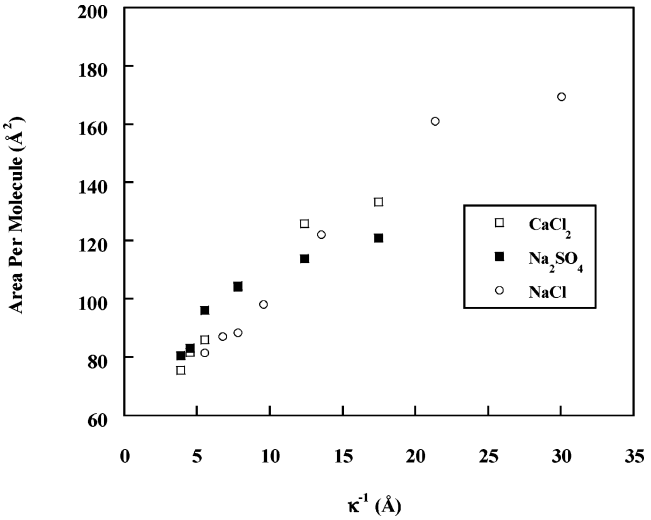

Figure 5. Variation of area per adsorbed surfactant molecule of C_{14}PB as a function of Debye screening length (κ^{-1}). Area occupied per molecule in absence of electrolyte is 244.2 Å^2. The initial concentrations of C_{14}PB were 0.5 mM, and the equilibrium time was taken for 1 h at 25 °C.

increasing the amount adsorbed with increasing electrolyte concentration. Since the sand is hydrophilic, adsorption of cationic surfactant initially occurs mainly by cation exchange[16,23] and a few with the hydrophobic bonding with the surface. In the presence of electrolyte, adsorbed surfactant molecules are placed densely due to increased lateral interactions between the tails (hydrophobic bonding), as electrical repulsion between the headgroups is weakened.

Indeed, as shown in Figure 5, the area per molecule estimated based on the measured specific adsorption increases linearly with the Debye screening length (κ^{-1}) and is almost independent of the type of electrolytes. The area occupied per molecule is calculated as

$$A_m = \frac{S \times 10^{26}}{}$$

where A_m is the area occupied per surfactant molecule in Å^2, S is the specific surface area of sand in m^2/g, and Γ is the amount of surfactant adsorbed at saturation in mol/g.

To investigate further the role of headgroup repulsion in the adsorption of alkyl-PB on sand, the electrostatic repulsion, Φ_R,

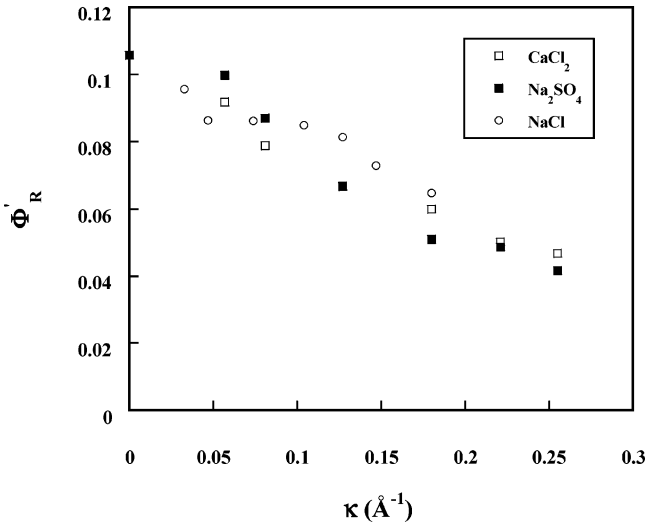

Figure 6. Variation of reduced potential energy (Φ_R') of $C_{14}PB$ as a function of Debye−Hückel parameter (κ). The initial concentrations of $C_{14}PB$ were 0.5 mM, and the equilibrium time was taken for 1 h at 25 °C.

among surfactant heads was estimated using the expression given by Verwey and Overbeek[24] for the electrostatic interaction between two charged spheres of radius *a* separated by a center-to-center distance *R*, namely,

$$\frac{\Phi_R}{a\epsilon\psi_0^2} = \frac{e^{-\kappa a(s-2)}}{s} \tag{4}$$

where ψ_0 is the surface potential and $s = R/a$. Using the area per molecule, A_m, calculated above, the equilibrium value of *s* can be estimated as $s_{eq} = R_{eq}/a$, where $R_{eq} = (4A_m/\pi)^{1/2}$ is the distance between two adsorbed surfactant molecules in a saturated monolayer. Thus, the reduced potential energy, Φ_R', at $R = R_{eq}$ can be expressed as

$$\Phi_R' = \frac{e^{-\kappa a(s_{eq}-2)}}{s_{eq}} \tag{5}$$

The role of headgroup repulsion can now be assessed, at least qualitatively, by considering the variation of Φ_R' as a function of κ, as shown in Figure 6. The strong linear correlation between Φ_R' and κ clearly indicates that headgroup repulsion decreases with increasing ionic strength, which is consistent with the observed adsorption behavior. In considering Figure 6, it is important to note that R_{eq} is dependent on ionic strength or κ. In principle, R_{eq} can be determined by minimizing the system free energy, which also includes other interactions such as van der Waals attractions among surfactant tails and those between the surfactant and the solid surface. As we have mentioned above, both the hydrophobic and electrical interactions are dependent on ionic strength, so R_{eq} is also dependent on ionic strength. Since headgroup repulsion appears to play a crucial role in the adsorption of alkyl-PB on sand, the concentration of the added anion (Cl^- and SO_4^{2-}) should also be an important parameter. Figure 7 depicts the concentration of surfactant on sand surface, calculated as $1/A_m$, as a function of $(\rho-)^{1/2}$, where $\rho-$ is the concentration of the added anion. Two features in Figure 7 are particularly noteworthy: (i) the system containing Na_2SO_4 has higher surface concentrations than the other two systems and (ii) the slopes of the fitted lines for $CaCl_2$ and Na_2SO_4 are almost identical. The values of the slopes of the fitted lines for Na_2SO_4, $CaCl_2$, and NaCl are 0.00038, 0.00038, and 0.00049, respectively, with >0.99 correlation coefficient.

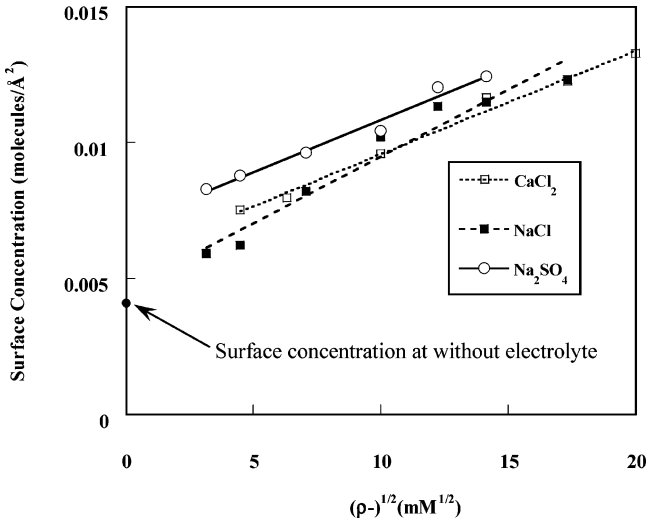

Figure 7. Effect of added anion concentration, $\rho-$, on the surface concentration of $C_{14}PB$. The initial concentrations of $C_{14}PB$ were 0.5 mM, and the equilibrium time was taken for 1 h at 25 °C. The lines are linear fit to experimental data.

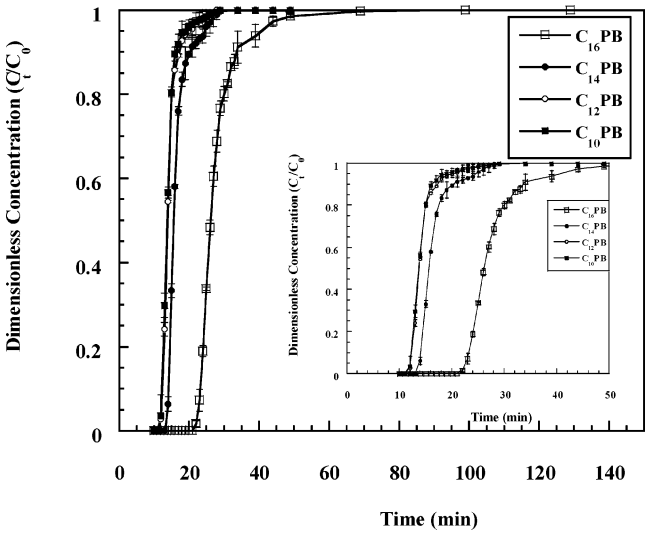

The divalent calcium ion will more effectively reduce the surface potential of sand than sodium ion at the same concentration, which would tend to reduce the surface concentration of surfactant molecules. On the other hand, the divalent sulfate ion is more effective in reducing the repulsion between surfactant headgroups than chloride ion at the same concentration, which will increase the surface concentration. While the higher surface concentrations in the Na_2SO_4 system suggest that the divalent anion is able to allow a closer arrangement of surfactants on the surface, the reason behind the slope similarity between the $CaCl_2$ and Na_2SO_4 systems is not clear. The effects of multivalent ions on surfactant adsorption at free surfaces have been studied previously (see, for example, refs 25 and 26 and references therein), but more detailed modeling may be required to delineate the effects of asymmetric electrolytes observed here, which is beyond the scope of the present study.

3.3. Effect of Surfactant Tail Length in Column Studies. Figure 8 shows the adsorption behavior of $C_{16}PB$, $C_{14}PB$, $C_{12}PB$, and $C_{10}PB$ at the same concentration of 1 mM under dynamic conditions. The results are presented as dimensionless concentration (ratio of outlet surfactant concentration to inlet concen-

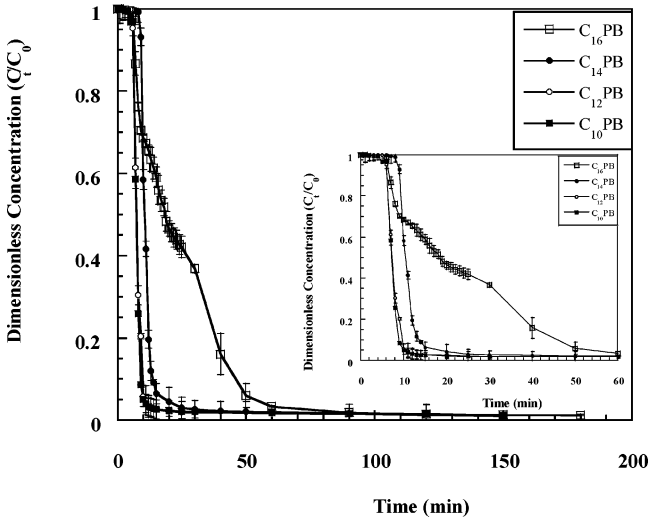

Figure 9. Desorption of $C_{16}PB$, $C_{14}PB$, $C_{12}PB$, and $C_{10}PB$ when eluted with pure water after adsorption at 1 mM inlet concentration and 25 °C. Inset shows the same plot at a smaller time scale.

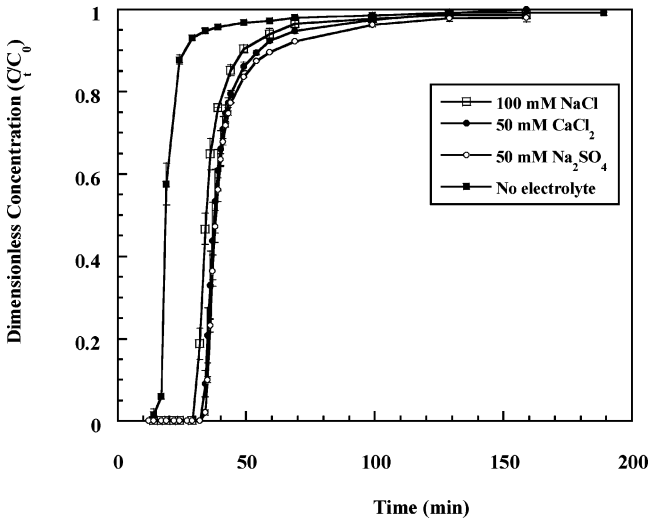

Figure 10. Adsorption of $C_{14}PB$ in the sand column at 0.5 mM inlet concentration and 25 °C in the presence of different background electrolytes.

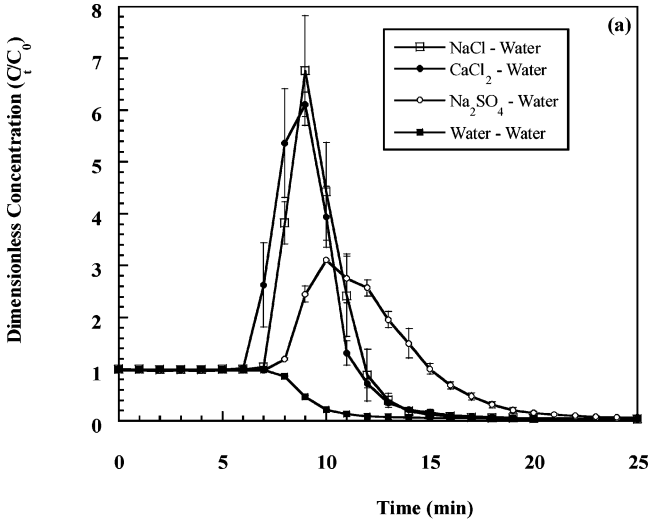

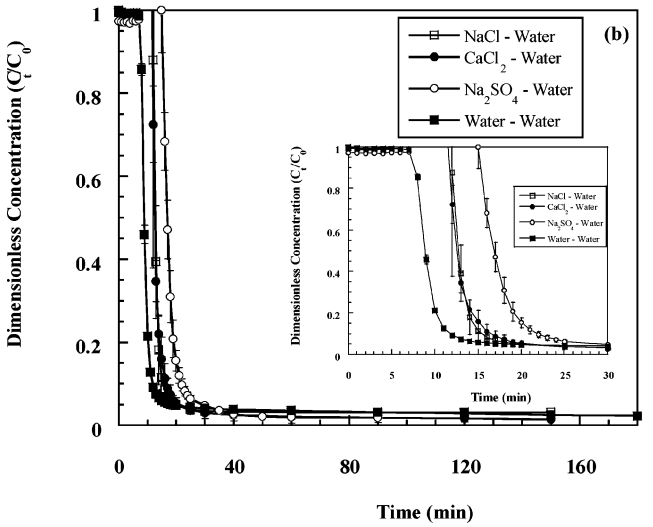

Figure 11. (a) Desorption of $C_{14}PB$ when eluted with pure water after adsorption at 0.5 mM inlet concentration of $C_{14}PB$ in the presence of electrolytes. (b) Desorption of $C_{14}PB$ when eluted with pure water after adsorption in the presence of electrolytes (excluding the peak). Inset shows the same plot at a smaller time scale. Experiments were carried out at 25 °C.

tration) vs time. As shown in the figure, the breakthrough curves follow the regular S-shape and the sequence of start of breakthrough is $C_{16}PB > C_{14}PB > C_{12}PB \approx C_{10}PB$. Note that, similar to the batch experiment, there is a considerable difference in the start of breakthrough between $C_{16}PB$ and $C_{14}PB$. This can be explained based on the batch adsorption isotherm in terms of the difference in the amount of surfactant adsorbed. More specifically, since the inlet concentration is very close to the equilibrium concentration at the saturation of $C_{16}PB$, the amount of surfactant adsorbed in the case of $C_{16}PB$ is much more than those for $C_{14}PB$, $C_{12}PB$, and $C_{10}PB$. Consequently, $C_{16}PB$ requires more pore volumes to initiate the breakthrough. In addition, since the inlet concentration is much lower than the equilibrium concentration at the saturation of $C_{12}PB$ and $C_{10}PB$, there is little difference in the amount adsorbed at that concentration in the batch, and the adsorption curves through the column are almost identical. Figure 9 shows the desorption curves for $C_{16}PB$, $C_{14}PB$, $C_{12}PB$, and $C_{10}PB$. No appreciable difference is observed between $C_{12}PB$ and $C_{10}PB$, and only a very small difference is found between these two and $C_{14}PB$. In all three cases, most of the surfactant molecules are eluted from the column within 15 to 20 min. On the other hand, a considerable difference is observed between $C_{16}PB$ and the other three surfactants. Since more $C_{16}PB$ surfactant molecules are adsorbed, more time (~60 min) is required for the surfactants to be eluted.

3.4. Effect of Electrolytes in Column Studies. Figure 10 shows the effect of NaCl, $CaCl_2$, and Na_2SO_4 on the adsorption of $C_{14}PB$ through the column. The concentrations of NaCl, $CaCl_2$, and Na_2SO_4 used were 100 mM, 50 mM, and 50 mM, respectively. As shown in the figure, in all three cases, breakthrough time is delayed compared to the case without electrolyte. This behavior is consistent with the batch experiments, which indicate that the amount adsorbed increases in the presence of electrolyte.

Figure 11 shows the desorption of surfactant when eluted with pure water after adsorption in the presence of different electrolytes. For simplicity, the data are labeled by the solutions used in the adsorption−desorption sequence. For example, "NaCl−water" denotes the case where adsorption was performed in the presence of 100 mM NaCl, followed by desorption with pure water. The electrolyte solutions used in this study were the same as noted above. Figure 11a shows that, after approximately one pore volume (7 min), there is a sudden increase in outlet surfactant concentration. The effect seen in Figure 11a

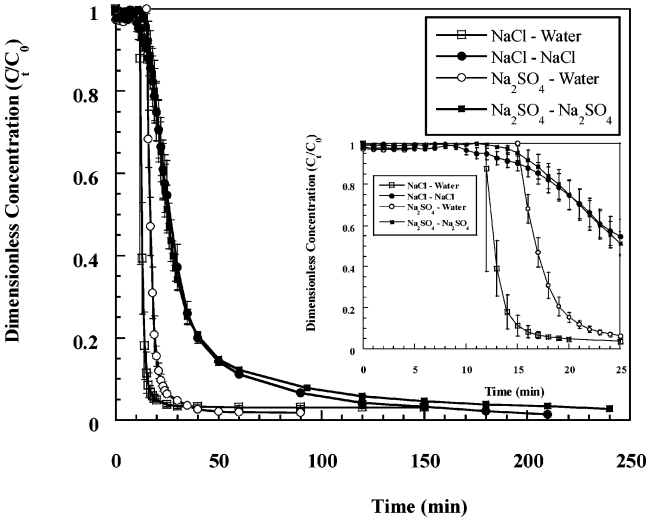

Figure 12. Desorption of C_{14}PB when eluted with pure water and in the presence of electrolytes after adsorption at 0.5 mM inlet concentration of C_{14}PB in the presence of electrolytes (excluding the peak). Inset shows the same plot at a smaller time scale. Experiments were carried out at 25 °C.

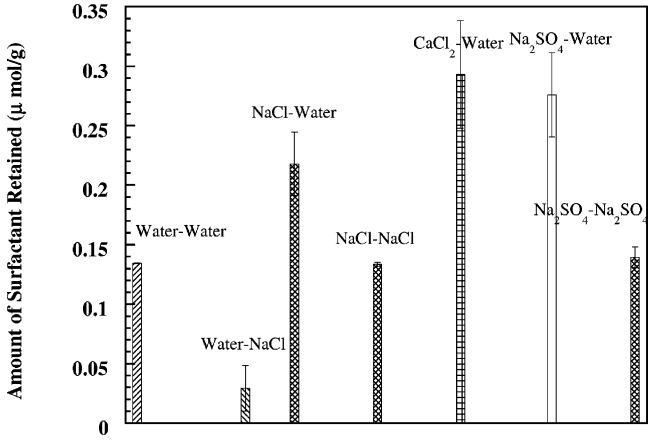

Figure 13. Amount of C_{14}PB retained in the sand column after desorption under different electrolyte conditions at 25 °C. The adsorption was performed at 0.5 mM inlet concentration of C_{14}PB in the presence and absence of electrolytes.

is basically the same principle of liquid chromatography. First the compounds are deposited on the stationary phase; then they are concentrated and eluted in a "pulse" by changing the eluent. The maximum peak height for NaCl−water and $CaCl_2$−water are very similar ($C_t/C_0 \approx 6-6.8$), but that for Na_2SO_4−water is significantly lower ($C_t/C_0 \approx 3$). The times required for maximum amount released are almost the same for all three electrolytes (9−10 min), but after the maximum desorption, the rate of desorption is lower for Na_2SO_4−water. The appearance of a peak in the desorption curve is consistent with the notion that adsorption in the presence of electrolytes is enhanced due to reduced repulsion between the adsorbed headgroups. More specifically, in the presence of electrolyte, more surfactant molecules were adsorbed because of a reduction in repulsion between the headgroups. When pure water was then injected into the column, the adsorbed surfactant molecules began to experience a stronger repulsive force similar to that without electrolyte. Consequently, the excess molecules adsorbed on the surface desorbed immediately, resulting in the observed increase in outlet surfactant concentration after one pore volume. This observation is further supported by other experiments, which will be discussed in a later paragraph (see Figure 12). The lower peak height of the Na_2SO_4–water desorption curve is probably caused by the higher valence of the anion. Since the divalent SO_4^{2-} ion may bridge between two adsorbed surfactant molecules, it may be more strongly bound with the adsorbed molecules, resulting in slower desorption and lower peak height. Figure 11b presents the same curves as in Figure 11a, but with a larger time scale and the peak excluded. The figure shows that, excluding the peaks, the curves are almost identical to that of the water−water system, where the peak is absent. This indicates that the excess amount of surfactants eluted during desorption is almost the same as the additional amount adsorbed in the presence of electrolytes.

Figure 12 compares the desorption curves for NaCl−water, Na_2SO_4−water, NaCl−NaCl, and Na_2SO_4−Na_2SO_4, excluding the peak. Note that no elution peak is found in the NaCl−NaCl and Na_2SO_4−Na_2SO_4 systems, and the rates of desorption in both cases are lower than those for the NaCl−water and Na_2SO_4−water systems. The lower rate of desorption can be understood by considering the fact that the adsorbed molecules are not experiencing any difference in electrostatic repulsion caused by a change in electrolyte concentration, and desorption is due to the surfactant concentration gradient between the solid surface and the bulk phase (pore space). The figure also shows the difference between the NaCl−NaCl and Na_2SO_4−Na_2SO_4 systems at a smaller time scale between 10 and 25 min, where the rate is lower for Na_2SO_4−Na_2SO_4, probably because of the difference in the valence of the counterions as noted above.

Figure 13 shows the amount of surfactant retained in the column after desorption under different conditions. Surfactant retention is an important factor in various applications. In soil remediation, for example, surfactant retention is not desirable because of environmental concerns, whereas retention is a key parameter in other applications such as soil modification for groundwater purification.[1] To determine the amount retained, 500 mL of 0.5 mM surfactant solution was passed through the column, followed by water or electrolyte solution until the outlet surfactant concentration became zero. The amount retained was calculated from the difference in inlet and outlet concentrations. Comparing the cases of water−water and water−NaCl (Figure 13), the water−NaCl system shows a very small amount of surfactant retained in the column. As we have seen before (Figure 4), the amount of surfactants increases in the presence of electrolyte mainly because of the reduction in repulsive force between the headgroups; the excess amount of adsorbed surfactant can be eluted easily by passing different eluent. The amount of surfactant retained after desorption is mainly determined by the electrostatic attraction between the negatively charged surfaces and the cationic surfactants. When desorption was performed in the presence of NaCl, the thickness of the electrical double layer on the sand surface was significantly reduced, resulting in a weaker electrostatic attractive force between the surface and the surfactant molecules and, therefore, a lower retention. The amounts retained for NaCl−NaCl and Na_2SO_4−Na_2SO_4 are similar and lower than those of NaCl−water and Na_2SO_4−water. We hypothesized that the observed results are due to the same reason as mentioned in the water−NaCl system.

In the presence of electrolyte, coion (positively charged ion) reduces the potential at the soil surface, which, in turn, reduces adsorption. On the other hand, counterion reduces the electrical double layer thickness around the surfactant heads, which reduces the repulsion between two adsorbed molecules. The results of this study show that adsorption is enhanced by increasing ionic strength, which indicates that the second effect is more predominant for cationic surfactant adsorption. In

addition to the reduction in electrostatic repulsion, when two surfactant molecules approach each other, hydrophobic interaction between the tails may also become more favorable, thus helping to enhance the adsorption.

In the application of surfactant flushing for in situ soil remediation, surfactant solutions are injected into the subsurface through injection wells.[16] Since soil contains different types of salt, the knowledge of the adsorption mechanisms in the presence of salt is very important. In particular, understanding the effects of electrolyte and surfactant tail length under static and dynamic conditions may help to (i) determine the suitability of cationic surfactants for the process, (ii) quantify the loss of surfactant due to adsorption, and (iii) develop mathematical models for predicting and analyzing the performance of this technology. Furthermore, the adsorbed cationic surfactant may be toxic to the pollutant-degrading bacteria,[27] which is another important reason for understanding surfactant retention in soil under different conditions.

4. Conclusion

The adsorption kinetics of four pyridinium bromide cationic surfactants with different tail lengths on sand show that the rate of adsorption is very high (70% of the saturation amount is adsorbed within 30 s) and the adsorption rates are almost the same for all four surfactants. Electrostatic interaction is a more important factor than surfactant tail length when adsorption occurs on an oppositely charged surface; for the three electrolytes considered in this study, NaCl, $CaCl_2$ and Na_2SO_4, specific adsorption increases with increasing ionic strength.

Column adsorption studies in the presence of electrolytes and desorption with pure water show a sudden peak in surfactant concentration after one pore volume, which can be explained by the increased adsorption in the presence of electrolytes due to a reduction in electrostatic repulsive force between the adsorbed molecules. The divalent counterion may bind strongly with the surfactant molecules, resulting in a lower rate of desorption. The amount of surfactant retained in the column is lower when desorption occurs in the presence of electrolyte instead of pure water, which can be attributed to the reduced attractive force between the surface and surfactant molecules.

Acknowledgment

This research was supported in part by the Natural Sciences and Engineering Research Council of Canada (NSERC), the Canada Foundation for Innovation (CFI), and the Nova Scotia Research and Innovation Trust Fund.

Literature Cited

(1) Boyd, S. A.; Lee, L. J.; Mortland, M. M. Attenuating organic contaminant mobility by soil modification. *Nature* **1988**, *333*, 345.

(2) Lee, J. F.; Crum, J. R.; Boyd, S. A. Enhanced retention of organic contaminants by soils exchanged with organic cations. *Environ. Sci. Technol.* **1989**, *23*, 1365.

(3) Chiou, C. T.; Porter, P. E.; Schmedding, D. W. Partition equilibriums of nonionic organic compounds between soil organic matter and water. *Environ. Sci. Technol.* **1983**, *17*, 227.

(4) Gao, Y.; Du, J.; Gu, T. Hemimicelle formation of cationic surfactants at the silica gel−water interface. *J. Chem. Soc., Faraday Trans. 1* **1987**, *83*, 2671.

(5) Wangnerud, P.; Berling, D.; Olofsson, G. Adsorption of alkyltrimethylammonium bromides on silica: Calorimetric study of effect of coions. *J. Colloid Interface Sci.* **1995**, *169*, 365.

(6) Atkin, R.; Craig, V. S. J.; Biggs, S. Adsorption kinetics and structural arrangements of cetylpyridinium bromide at the silica−aqueous interface. *Langmuir* **2001**, *17*, 6155.

(7) Atkin, R.; Craig, V. S. J.; Wanless, E. J.; Biggs, S. The influence of chain length and electrolyte on the adsorption kinetics of cationic surfactants at the silica−aqueous solution interface. *J. Colloid Interface Sci.* **2003**, *266*, 236.

(8) Zajac, J.; Trompette, J. L.; Partyka, S. Adsorption of cationic surfactants on a hydrophilic silica surface at low surface coverages: Effects of the surfactant alkyl chain and exchangeable sodium cations at the silica surface. *Langmuir* **1996**, *12*, 1357.

(9) Xu, S.; Boyd, S. A. Cation exchange chemistry of hexadecyltrimethylammonium in a subsoil containing vermiculite. *Soil Sci. Soc. Am. J.* **1994**, *58*, 1382.

(10) Boyd, S. A.; Mortland, M. M.; Chiou, C. T. Sorption characteristics of organic compounds on hexadecyltrimethylammonium-smectite. *Soil Sci. Soc. Am. J.* **1988**, *52*, 652.

(11) Xu, S.; Boyd S. A. Cationic surfactant adsorption by swelling and nonswelling layer silicates. *Langmuir* **1995**, *11*, 2508.

(12) Fan, A.; Somasundaran, P.; Turro, N. J. Adsorption of alkyltrimethylammonium bromides on negatively charged alumina. *Langmuir* **1997**, *13*, 506.

(13) Goloub, T. P.; Koopal, L. K. Adsorption of cationic surfactants on silica. Comparison of experiment and theory. *Langmuir* **1997**, *13*, 673.

(14) Grim, R. E.; Allaway, W. H.; Cuthbert, F. L. Reaction of different clay minerals with some organic cations. *J. Am. Ceramic Soc.* **1947**, *30*, 137.

(15) Cowan, C. T.; White, D. Mechanism of exchange reactions occurring between sodium montmorillonite and various *n*-primary aliphatic amine salts. *Trans. Faraday Soc.* **1958**, *54*, 691.

(16) Xu, S.; Boyd, S. A. Cationic surfactant sorption to a vermiculitic subsoil via hydrophobic bonding. *Environ. Sci. Technol.* **1995**, *29*, 312.

(17) Subramanian, V.; Ducker, W. A. Counterion effects on adsorbed micellar shape: Experimental study of the role of polarizability and charge. *Langmuir* **2000**, *16*, 4447.

(18) Zhu, L.; Feng, S. Synergistic solubilization of polycyclic aromatic hydrocarbons by mixed anionic−nonionic surfactants. *Chemosphere* **2003**, *53*, 459.

(19) Kaewprasit, C.; Hequet, E.; Abidi, N.; Gourlot, J. P. Application of methylene blue adsorption to cotton fiber specific surface area measurement. Part I. Methodology. *J. Cotton Sci.* **1998**, *2*, 164.

(20) Iler, R. K. *The chemistry of silica*; Wiley: New York, 1979.

(21) Johnson, P. R.; Sun, N.; Elimelech, M. Colloid transport in geochemically heterogeneous porous media: Modeling and measurements. *Environ. Sci. Technol.* **1996**, *30*, 3284.

(22) Paria, S.; Khilar, K. C. A review on experimental studies of surfactant adsorption at the hydrophilic solid−water interface. *Adv. Colloid Interface Sci.* **2004**, *110*, 75.

(23) Xu, S.; Boyd, S. A. Alternative model for cationic surfactant adsorption by layer silicates. *Environ. Sci. Technol.* **1995**, *29*, 3022.

(24) Verwey, E. J. W.; Overbeek, J. Th. G. *Theory of the Stability of Lyophobic Colloids*; Elsevier: Amsterdam, The Netherlands, 1948.

(25) Gilányi, T.; Varga, I.; Mészáros, R. Specific counterion effect on the adsorption of alkali decyl sulfate surfactants at air/solution interface. *Phys. Chem. Chem. Phys.* **2004**, *6*, 4338.

(26) Faure, N.; Bouloussa, O.; Rondelez, F. Influence of multivalent counterions adsorption on Langmuir films. *Eur. Phys. J. E* **2004**, *15*, 149.

(27) Nye, J. V.; Guerin, W. F.; Boyd, S. A. Heterotrophic activity of microorganisms in soils treated with quaternary ammonium compounds. *Environ. Sci. Technol.* **1994**, *28*, 944.